SFI Sustainable Forestry Implementation

With support from Federal Ministry of Food and Agriculture by decision of the German Bundestag

Forest Policy Report **SFI/2023**

Remote Sensing Based Forest Inventory of Ukraine (RS-Inventory): Case Study for Sumy Administrative Oblast

Viktor Myroniuk

Kyiv, August 2023

About the Project "Sustainable Forestry Implementation" (SFI)

The project "Technical Support to Forest Policy Development and National Forest Inventory Implementation" (SFI) is a project established in the framework of the Bilateral Cooperation Program (BCP) of the Federal Ministry of Food and Agriculture of Germany (BMEL) with the Ministry of Environment and Natural Resources of Ukraine (MENR). It is a continuation of activities started in the forest sector within the German-Ukrainian Agriculture Policy Dialogue (APD) forestry component.

The Project is implemented based on an agreement between GFA Group, the general authorized executor of BMEL, and the State Forest Resources Agency of Ukraine (SFRA) since October 2021. On behalf of GFA Group, the executing agencies - Unique land use GmbH and IAK Agrar Consulting GmbH - are in charge of the implementation jointly with SFRA.

The project aims to support sustainable forest management planning in Ukraine and has a working focus on the results in the Forest Policy and National Forest Inventory.

Author

Viktor Myroniuk

Contacts

Troitska Str. 22-24,
Irpin, Kyiv region
+38 (067) 964 77 02

CONTENT

LIST OF ABBREVIATIONS

AGB Above Ground Biomass
BA Basal Area
CI Confidence Interval
FMP Forest Management and Planning
FNF Forest/non-forest
GEE Google Earth Engine
GFF Green Forest Floor
GNN Gradient Nearest neighbor
GREG Generalized Regression
GSV Growing Stock Volume
LC Land Cover
LOO Leave-One-Out
MSI MultiSpectral Instrument
NBR Normalized Burn Ratio
NDVI Normalized Difference Vegetation Index
NFI National Forest Inventory
OA Overall Accuracy
OWV Other Woody Vegetation
PA Producer's Accuracy
RF Random Forest
RS Remote Sensing
SRTM Shuttle Radar Topography Mission
TCT Tasselled Cap Transformation
TPI Topography Position Index
TS Time Series
UA User's Accuracy

SUMMARY

National forest inventory (NFI) is an important tool for forest resources assessment that supports national forest policy. Implementation of the NFI of Ukraine is highly restricted due to the ongoing Russian invasion that made it impossible to collect all necessary field data. Thus, only remote sensing technologies can provide auxiliary information for areas that were not visited during field campaigns. What differentiates the situation in Ukraine is that significant territories are not controlled by the Government of Ukraine, located in the vicinity of front lines, or contaminated by unexploded ordnance/land mines. In line with these issues, a group of international and national short-term experts developed a Concept Study for the implementation of the NFI over Ukraine using collected sample plot data, forest management and planning (FMP) information, in combination with aerial photos and satellite imagery (RS-Inventory).

The concept of the RS-Inventory assumes utilization of all available NFI data collected in 2021–2023 using a regular national-wide sampling design. For regions of Ukraine that lack such plots' data, characteristics of forest stands are obtained from the most recent (<5 years) FMP data sets. These include polygonal coverage with boundaries of forest stands and associated forest attributes. Combining both data sets, i.e., NFI and FMP data, and satellite observations provides the foundation for the implementation of the RS-Inventory over Ukraine.

This study is aimed to investigate the potential of the RS-Inventory within the Sumy region of Ukraine as a necessary step to implementing the methodology at a larger spatial scale. The objectives of the study were as follows:

- Detailed description of the potential methodology of combined use of NFI, FMP, and satellite data, including error analysis.
- Testing the performance of a proposed mapping approach using different types of satellite data, i.e., Landsat vs Sentinel.
- Evaluation the role of the FMP data to improve the predictive performance of the approach in terms of mapping detailed forest attributes.
- Demonstrating the potential of the RS-Inventory for estimation of aboveground biomass and carbon in forest stands.
- Elaborate on final output tables that can be produced in RS-Inventory.

1. INPUT DATA AND METHODOLOGY

1.1. REFERENCE DATA

Three main sources of reference data were used in the study: 1) NFI sample plots, 2) FMP data, and 3) visually interpreted high-resolution imagery at NFI plot locations. The first two data sets were used to train predictive models to map forest attributes. These data were collected within forested areas and cannot be used to produce binary forest/non-forest (FNF) maps. Thus, the NFI sampling grid was visually interpreted using all plot locations to provide the necessary information for such classification.

1.1.1. NFI SAMPLE PLOTS

The reference data included the list of forest attributes estimated at sample plot locations according to the proposed structure in the Concept Study (Table 3). The Centre of NFI provided this data set in the form of MS Excell spreadsheets. Species basal areas (BA) were calculated using the total BA at the sample plot and provided the percentage of the species share. According to provided sample plot data, 28 tree species were identified within the Sumy region. The previous studies (e.g., Myroniuk et al., 2022) demonstrated the higher efficiency of mapping species groups than individual species, thus BAs were summarized for each sample plot (Table 1).

Table 1. Species groups in the Sumy region

Species group	Scientific species name
Oak	*Quercus robur* L.
Pine	*Pinus sylvestris* L., *Picea abies* L.
Maple	*Acer platanoides* L.
Linden	*Tilia cordata* Mill.
Birch	*Betula pendula* Roth.
Ash	*Fraxinus excelsior* L., *Fraxinus viridis* F.Michx
Poplar	*Populus tremula* L., *Populus alba* L.
Alder	*Alnus glutinosa* (L.) Gaerth, *Alnus incana* (L.) Moench
Willow	*Salix alba* L., *Salix fragilis* L., *Salix caprea* L.
Other hardwood deciduous species	*Acer campestre* L., *Acer negundo* L., *Acer tataricum* L., *Juglans nigra* L., *Querqus borealis* Michx., *Robinia pseudoacacia* L., *Ulmus minor* Mill.
Other rare species	Rare species of genus *Malus, Pirus, Crategus*

The initial data set contained information on 166 stands sampled at 145 unique locations. To eliminate the mixed pixel issues, i.e., when plots straddle different forest stands, the study utilized only those plots that were completely within the same forest stand (Fig. 1). Thus, only 145 NFI plots were used in further analysis.

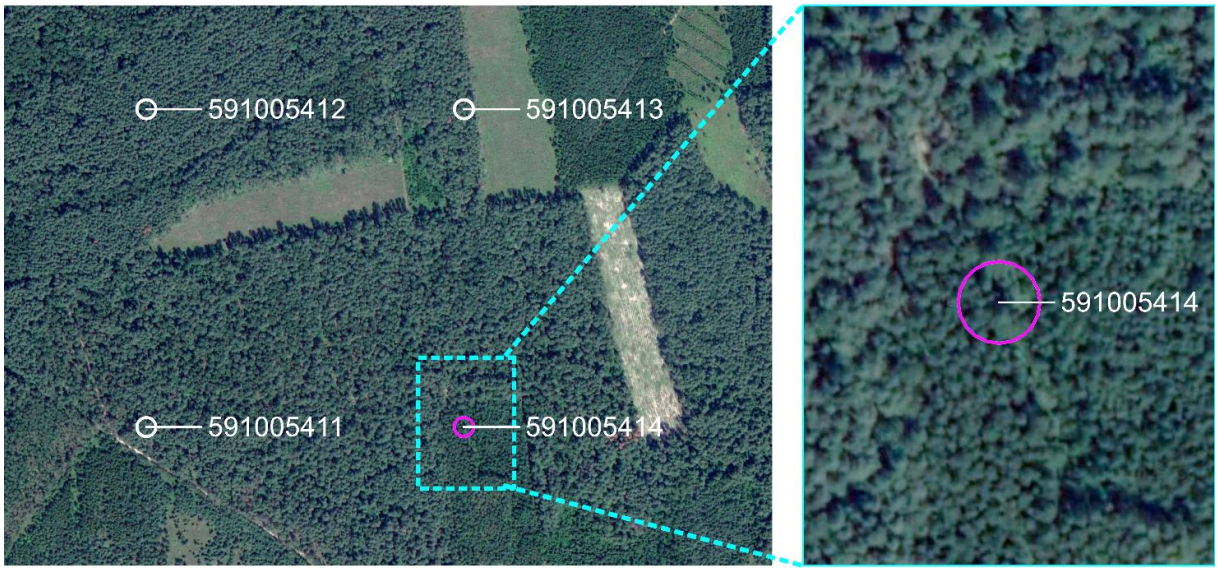

Figure 1. Example showing the issue when the plot (ID = 591005414) straddle different forest stands. Circles represent sample plots of 500 m² (plot radius = 12.62 m): white – plots located within one forest stands, magenta – plot located within two different forest stands.

1.1.2. FMP reference information

FMP data represent a subset of forest stands that are within 50-m buffer zone of NFI plots (Fig. 2). The FMP data included a) a GIS layer (ESRI shape-file) with boundaries of forest stands, and b) a table (MS Excel spreadsheet) with selected forest attributes that can be used to obtain the same data structure as it was provided for NFI plots.

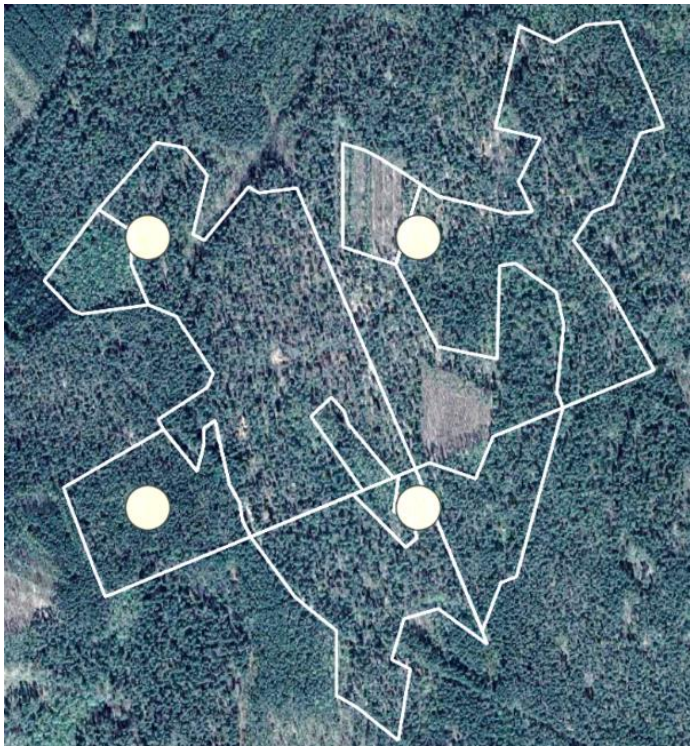

Figure 2. Subset of FMP data intersecting NFI sample plots within 50-m buffer.

These two data sets can be linked using a unique plot identifier (key field) in the following format – OOEEEEDDBBBPPPS. The key field can be assembled using the following stand attributes:

- OO – the code of the Sumy oblast (two digits, 59)
- EEE – the code of forest enterprise (three digits, e.g., 060)
- DD – the code of forest district (two digits, e.g., 01)
- BBB – forest block (three digits, e.g., 039)
- PPP – forest polygon (three digits, e.g., 020)
- S – forest sub-polygon (one digit, e.g., 0).

In contrast to NFI plots that contain estimates of species BA, FMP data do not have such information. Thus, species BAs were calculated using yield tables of fully-stocked forest stands (Bilous et al., 2020):

$$BA_{sp} = BA_{1.0} \cdot \frac{GSV_{sp}}{GSV_{1.0}},$$

where BA_{sp} – BA for given species, $m^2 \cdot ha^{-1}$; $BA_{1.0}$ – BA of fully-stocked (i.e., normal stand with relative stocking = 1.0) from yield tables, $m^2 \cdot ha^{-1}$; GSV_{sp} – growing stock volume (GSV) for given species from FMP data, $m^3 \cdot ha^{-1}$; $GSV_{1.0}$ – the relevant GSV of fully-stocked forest stand from yield tables, $m^3 \cdot ha^{-1}$.

The yield tables use stand height as an input variable to obtain estimates of $BA_{1.0}$ and $GSV_{1.0}$ for given species. It is worth noting, that yield tables in Ukraine were compiled only for the main forest-forming species. BAs for other species we calculated using yield tables for corresponding substitute species (Table 2).

Stand densities (N_{sp}) were calculated using average diameter for given species and estimated BA_{sp}:

$$N_{sp} = 40000 \cdot \frac{BA_{sp}}{\pi \cdot D_{sp}^2},$$

where D_{sp} – average stand diameter for given species from the FMP data set, cm; π – 3.1416.

Table 2. Substitute species used to estimate BA using yield tables

Scientific species name	Species code	Code of substitute species
Robinia pseudoacacia L.	202805	202805
Betula pendula Roth.	302620	302620
Ulmus minor Mill.	202520	202200
Salix alba L.	304403	304400
Salix fragilis L.	304410	304400
Alnus glutinosa (L.) Gaerth.	304110	304110
Ulmus laevis Pall.	202505	202200
Quercus robur L.	202080	202080[1]
Quercus rubra L.	202050	202080[2]
Acer platanoides L.	202430	202200
Acer campestre L.	202433	202200
Acer negundo L.	202450	202200
Tilia cordata Mill.	304235	202080[3]
Populus tremula L.	304000	304000
Pinus sylvestris L.	100150	100150
Populus alba L.	304305	304300
Populus Canadensis Moench	304318	304300
Populus nigra L.	304345	304300
Malus sylvestris L.	513410	202200
Picea abies (L.) Karst.	100215	100215
Fraxinus excelsior L.	202325	202325
Fraxinus pennsylvanica L.	202310	202325
Carpinis betulus L.	202200	202200

1.1.3. Visual interpretation of the NFI data

The Collect Earth plugin (Bey et al., 2016) for Google Earth Engine was used in the visual photo-interpretation of NFI sample plots (Table 3, Fig. 3). The forest in the interpretation was defined as treed area > 0.1 ha with canopy cover > 30%.

Table 3. Distribution of sample plots between land cover (LC) categories

Land cover	Frequency
Forest	147
Other woody vegetation (OWV)	55
Grassland	98
Cropland	409
Wetland	33
Water	13
Urban	21
Total	*776*

[1] Planted seed stands.
[2] Coppice stands.
[3] Natural seed stands.

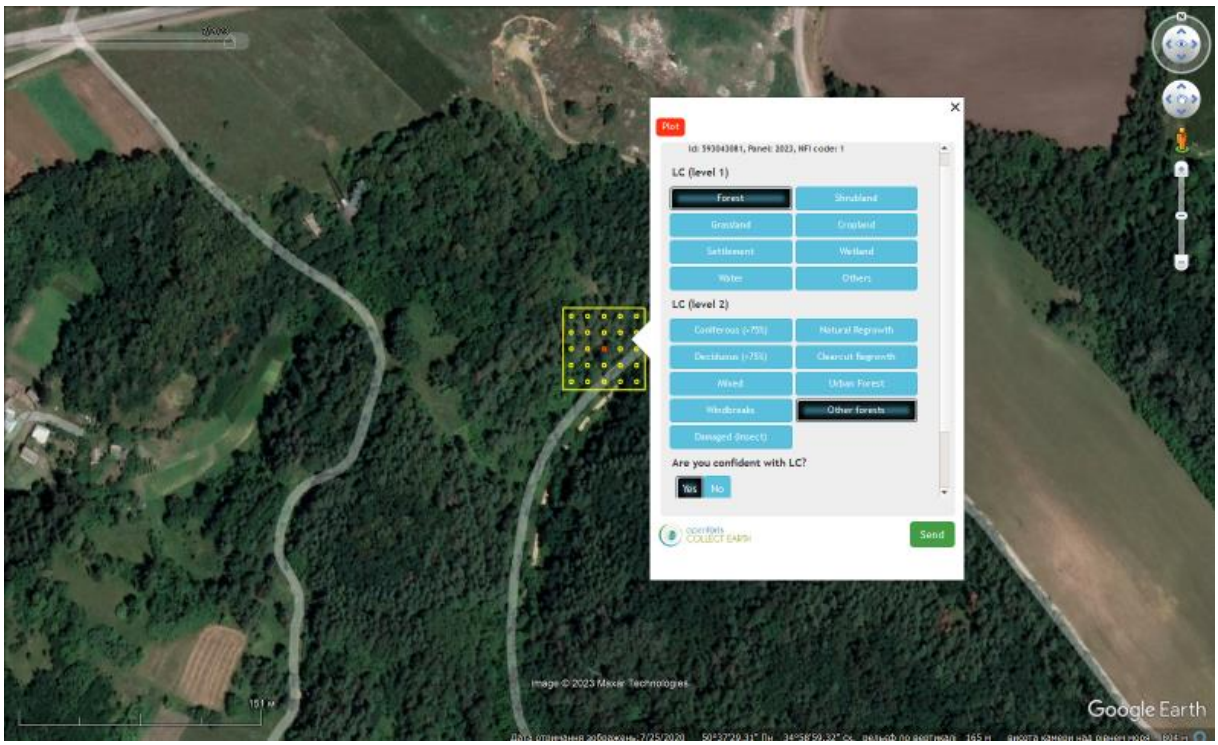

Figure 3. The user interface of the Collect Earth used in the photo-interpretation.

Historical Google Earth Pro imagery made it possible to track vegetation phenology which improved the interpretation of similar vegetation types. This was important to separate croplands and wetlands from grasslands.

1.2. Satellite time series

This study used both Landsat and Sentinel 2 satellite time series (TS) within the time range for which both data sets were available (i.e., March 2017 – June 2023). The study used all available surface reflectance imagery delivered as Google Earth Engine (GEE) (Gorelick et al., 2017) collections of Landsat 7-9, Collection 1, Tier 1 and harmonized Sentinel 2 MSI, Level 2A. Clouds, cloud shadows, and snow on Landsat images were screened using pixel quality attributes generated from the CFMask algorithm (Foga et al., 2017) and provided with QA_PIXEL band. High-quality clear observations from Sentinel TS were selected using the Scene Classification (SCL) band classes. In addition to the original spectral bands, the first three primary components (brightness, greenness, and wetness) of the Tasseled-Cap transformation (TCT) (Crist & Cicone, 1984), the normalized burn ratio (NBR) (Key & Benson, 2006), and Normalized Difference Vegetation Index (NDVI) were added to the image collections.

Landsat image collection was prepared at 30-m spatial resolution. Sentinel image collection was resampled to 20-m and 10-m resolutions.

1.3. Environmental variables

The study used additional environmental variables to improve the performance of predictive models (Fig. 4). These variables included elevation and topography position index (TPI) (Weiss, 2001) extracted from the 90-m Shuttle Radar Topography Mission (SRTM), mean annual precipitation and maximum temperature in July (Abatzoglou et al., 2018).

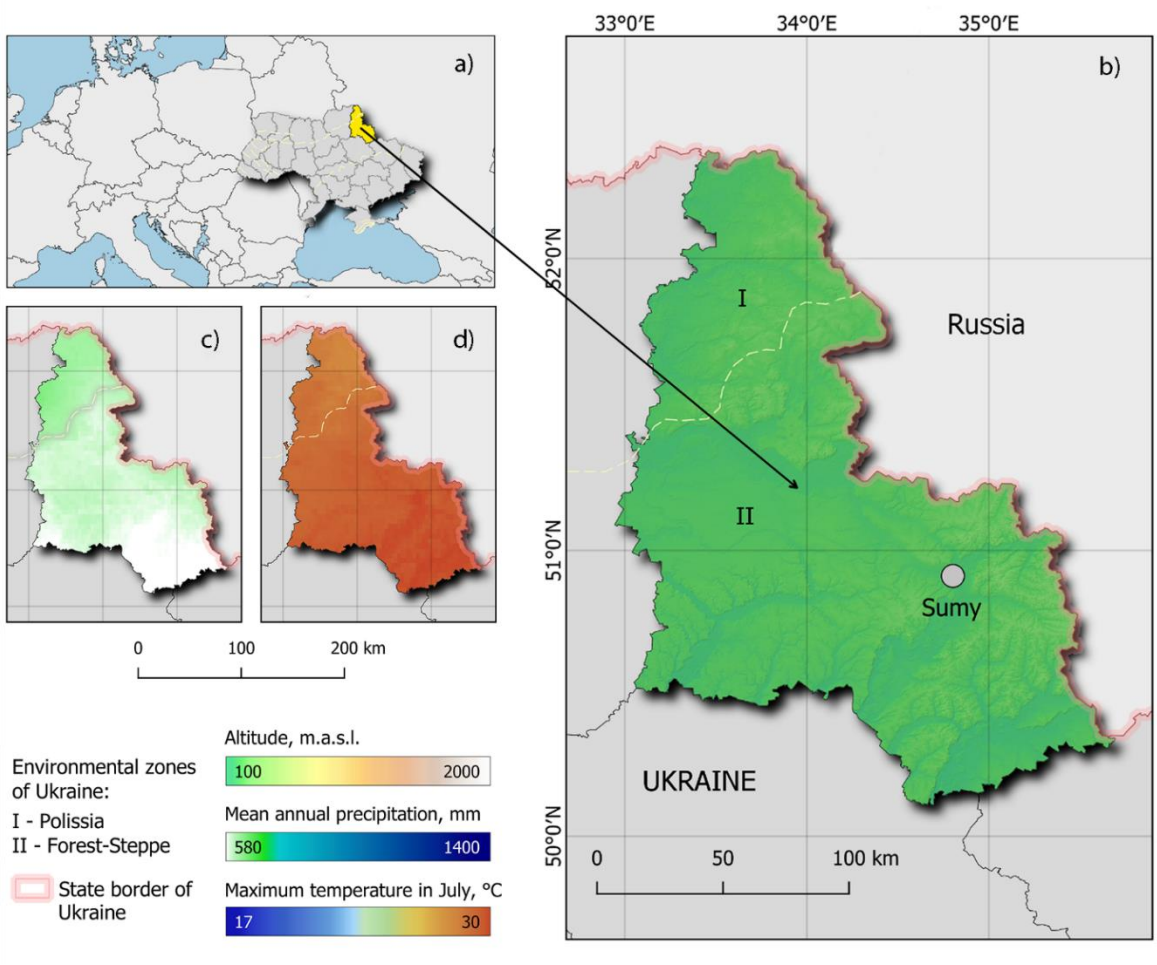

Figure 4. Location of the Sumy administrative oblast (a) along with environmental gradients: (b) elevation, (c) mean annual precipitation, (d) maximum temperature in July, °C.

1.4. Biomass and carbon models

Above ground biomass (AGB) and carbon stock were estimated for every forest stand using allometric equations (Bilous et al., 2017) (Annex 1). These equations use stands attributes (species, age, site index, relative stocking) to calculate forest live biomass. The carbon content in stems and branches was equal to 50% of the biomass, and 49% in crown foliage, understory, and green forest floor (GFF) (Matsala et al., 2023).

1.5. Processing workflow

Data processing workflow utilized the GEE cloud-computing that accelerated many steps of image processing. In addition, Quantum GIS and R software were used for data preparation.

1.5.1. Segmentation of satellite TS

Apart from many applications that utilize seasonal image mosaics (e.g., monthly or yearly), this study used temporally smoothed satellite TS. Temporal segmentation was performed using the Continuous Change Detection and Classification (CCDC) algorithm (Zhu & Woodcock, 2014). This approach is based on a harmonic regression capturing cyclic patterns of spectral reflectance in line with the vegetation phenology throughout the year. The CCDC algorithm uses all available clear pixel-level observations and splits TS into consecutive segments that correspond to stable spectral trajectories without LC change. The harmonic model coefficients can create a synthetic image for any date for which TS are available or used as predictor variables in classification.

The image collections were segmented using all available spectral bands, three components of TCT, NBR, and NDVI. The CCDC algorithm used default settings regarding probability thresholds to change detection, a minimal number of observations to flag changes, etc. (Zhu & Woodcock, 2014).

Regarding the large volume of information to be processed, the CCDC segmentation was performed for 0.5×1-degree tiles seamlessly covering the Sumy region (Fig. 5).

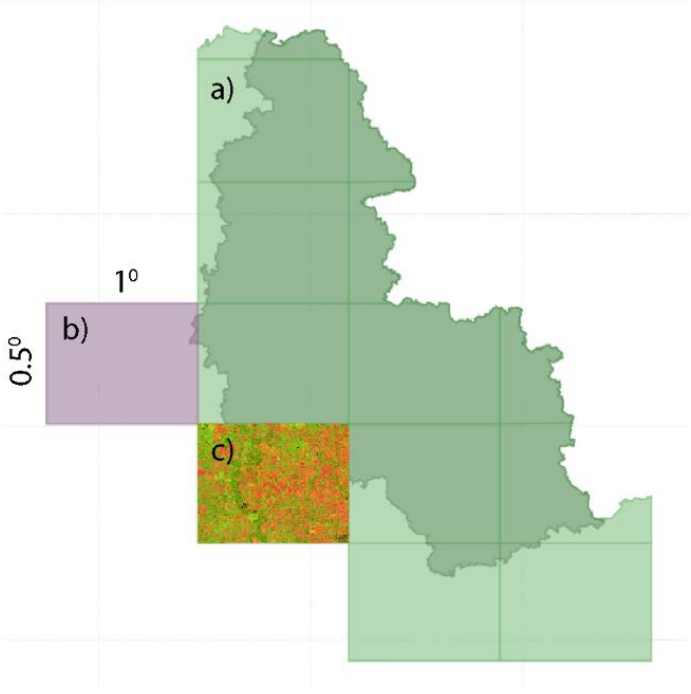

Figure 5. Regular 0.5×1-degree grid covering Sumy region: (a) tiles intersecting the boundary of the Sumy region; (b) the selected tile to be processed; (c) fitted synthetic image within the processed tile.

1.5.2. Mapping forested area

The forested area was mapped using Random Forest (RF) classifier (Breiman, 2001). Similarly to the previous study (Myroniuk et al., 2022), only spectral variables were used in the classification that included synthetic values of spectral bands (brightness, greenness, wetness components of the TCT, and NBR) predicted for the start (April 15), middle (June 15), and end (October 15) of a leaf-on period. These variables were augmented with coefficients of the CDDC harmonic models and derivations (phase, amplitude, and density of observations

per segment). Dates of image interpretations for all NFI plots were intersected with corresponding segments of the CCDC image. The RF models were trained independently for Landsat and two Sentinel (10-m and 20-m resolutions). Then, it was applied to a target year (2022) to obtain LC maps (see Table 3). FNF maps were extracted after re-classification into binary raster.

1.5.3. Mapping forest attributes

Forest attributes were mapped using the Gradient Nearest Neighbor (GNN) imputation (Myroniuk et al., 2022; Ohmann & Gregory, 2002). This approach is a multivariate prediction technique that can characterize a plant community structure as a cohesive unit, i.e., simultaneously predict combinations of different forest variables. The GNN model was built using the same list of predictor variables as in the case of the RF model. As response variables, per hectare values of total BA as well as BAs of species groups were used (see Table 1). Predictions for each target forest attribute were made using three nearest neighbors. Once species BAs were predicted, a threshold value of BA > 1 m^2 was applied to generate species presence/absence maps. Maps of dominant species (by BA) were developed using predicted BAs at pixel level.

1.6. Map accuracy assessment

Accuracies of the RF models were tested using leave-one-out (LOO) cross-validation. Following this procedure, the RF was trained on all data (776 iterations) except one observation used in the accuracy assessment. Obtained lists of observed and predicted values were used to construct confusion matrices using "good practices" protocol (Olofsson et al., 2014). The RF models were assessed using 95% confidence intervals (CI) for estimates of producer's (PA), user's (UA), and overall (OA) accuracies.

The accuracy of the GNN models was evaluated using the modified LOO approach based on three independent nearest neighbors (Ohmann & Gregory, 2002) excluding collocated plots in the same cluster. R^2 was used to report on predictive performance of the models for continuous values of BA, while the binary forecast of species presence/absence was evaluated using Cohen's kappa coefficient.

1.7. Estimation procedure

1.7.1. Estimating area

A forested area obtained directly from a map can differ from the actual area due to confusion between mapped classes. Once the confusion matrix is constructed, an error-adjusted estimator of the area can be used. Along with area estimation, confidence intervals for the forested area can be also provided to quantify the uncertainties of estimates. This study fully followed a "good practice" estimation procedure to quantify forested area and associated uncertainties (Olofsson et al., 2014).

1.8. Model-assisted estimation of forest attributes

1.8.1. Estimating area

A forested area obtained directly from a map can differ from the actual area due to confusion between mapped classes. Once the confusion matrix is constructed, an error-adjusted estimator of the area can be used. Along with area estimation, confidence intervals for the forested area can be also provided to quantify the uncertainties of estimates. This study fully followed a "good practice" estimation procedure to quantify forested area and associated uncertainties (Olofsson et al., 2014).

1.8.2. Model-assisted estimation of forest attributes

The generalized regression (GREG) estimator represents a class of model-assisted estimators that uses auxiliary variables for all population units and an assisting model to calibrate the estimator. The GREG is composed of the mean of the predicted values over the population and the model residuals (calculated using a sample). The estimation of mean values of forest attributes and corresponding variances was based on the tutorial developed for applications in forest inventory (McConville et al., 2020). Calculation of the standard error of the estimate as the square root of variance were used for the presentation of uncertainties. Confidence intervals were constructed at 95% level using t = 1.96.

GREG estimator:

$$\hat{\mu}_y = \frac{1}{n}\sum_{i\epsilon S}\left(y_i - \hat{m}(x_i)\right) + \frac{1}{N}\sum_{i\epsilon U}\hat{m}(x_i).$$

GREG variance:

$$\hat{V}(\hat{\mu}_y) = \left(1 - \frac{n}{N}\right)\frac{1}{n}\frac{1}{n-1}\sum_{i\epsilon S}\left(y_i - \hat{m}(x_i)\right)^2.$$

Confidence interval of model-assisted mean:

$$\hat{\mu}_y \pm t_{(n-1;1-\alpha/2)} \cdot \sqrt{\hat{V}(\hat{\mu}_y)},$$

where N – finite number of the population U units (pixels); n – number of selected units (plots) for the sample S; y_i – observed value for *i*-th unit; $\hat{m}(x_i)$ – predicted value for *i*-th unit given auxiliary data x; $t \approx 2$ for a 95% confidence interval.

2. RESULTS

2.1. Forested area

The forested area for the Sumy region was extracted from the corresponding LC map (Figure. 6). Confusion matrices showed that the classification models among Landsat and Sentinel TS exhibited similar characters of errors. All TS were able to correctly classify (main diagonals of error matrices) nearly equal proportions of the total area. The errors of forest classification are mostly explained by confusion with OWV and grasslands (with trees). It is also worth noting that the accuracy assessment presented in Tables 4-7 were obtained using only those samples for which LC were assigned with a high level of confidence during the photointerpretation (575 plots, see Figure 3).

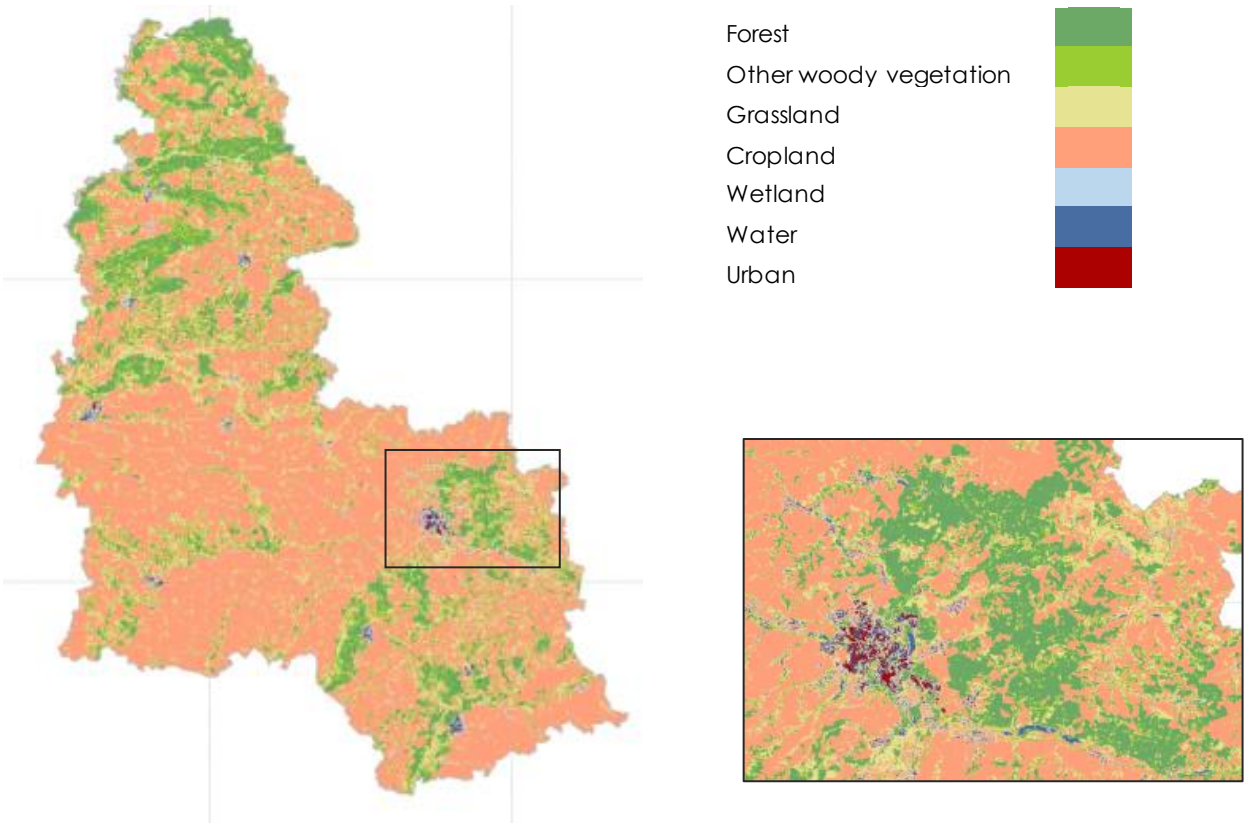

Figure 6. LC within the Sumy region (2022) extracted from Sentinel 2 (20-m) TS.

In general, accuracies were higher for Sentinel 2 than for Landsat TS. The smaller pixel size of Sentinel 2 data allowed us to map more forests. This can be explained by patchiness of forests, specifically narrow shelterbelts, which cannot be mapped from Landsat imagery. Regarding obtained results and required volume to store datasets for the region on the GEE platform (Landsat (30-m) ~50Gb; Sentinel 2 (20-m) ~110 Gb; Sentinel 2 (10-m) ~425 Gb), the selection of Sentinel 2 (20-m) seems to be more reasonable at the scale of the Ukraine.

Table 4. Confusion matrix with cell entries expressed in terms of proportion of total area (Olofsson et al., 2014) obtained for Landsat (30-m) TS

	Reference								Mapped area, thousand ha
Map	Forest	OWV	Grass-land	Crop-land	Wet-land	Water	Urban	Total	
Forest	**0.213**	0.019	0.002	0	0	0	0	0.235	559.8
OWV	0.008	**0.016**	0.014	0	0.003	0	0.003	0.044	103.8
Grassland	0	0.016	**0.063**	0.006	0.003	0	0.005	0.093	222.5
Cropland	0.002	0	0.01	**0.570**	0.010	0	0.003	0.596	1420.0
Wetland	0	0	0	0	**0.013**	0	0	0.013	31.0
Water	0	0	0	0	0	**0.005**	0	0.005	12.7
Urban	0	0	0	0	0	0	**0.014**	0.014	34.3

Table 5. Confusion matrix with cell entries expressed in terms of proportion of total area (Olofsson et al., 2014) obtained for Sentinel 2 (20-m) TS

	Reference								Mapped area, thousand ha
Map	Forest	OWV	Grass-land	Crop-land	Wet-land	Water	Urban	Total	
Forest	**0.235**	0.015	0	0	0.004	0	0	0.254	606.1
OWV	0	**0.024**	0.006	0	0.003	0	0.003	0.036	85.3
Grassland	0.002	0.014	**0.069**	0.005	0.003	0	0.005	0.098	233.5
Cropland	0.002	0.003	0.013	**0.558**	0.007	0	0.007	0.589	1404.0
Wetland	0	0	0.002	0	**0.005**	0	0	0.006	14.9
Water	0	0	0	0	0	**0.006**	0	0.006	13.6
Urban	0	0.001	0	0	0	0	**0.010**	0.011	26.2

Table 6. Confusion matrix with cell entries expressed in terms of proportion of total area (Olofsson et al., 2014) obtained for Sentinel 2 (10-m) TS

	Reference								Mapped area, thousand ha
Map	Forest	OWV	Grass-land	Crop-land	Wet-land	Water	Urban	Total	
Forest	**0.232**	0.015	0	0	0.002	0	0	0.249	594.0
OWV	0.005	**0.016**	0.008	0	0.005	0	0	0.034	81.3
Grassland	0.002	0.015	**0.071**	0.003	0.007	0	0.007	0.105	250.2
Cropland	0	0.003	0.008	**0.565**	0.002	0	0.007	0.585	1394.9
Wetland	0	0.001	0.001	0	**0.006**	0	0	0.009	20.7
Water	0	0	0	0	0	**0.006**	0	0.006	13.9
Urban	0	0.001	0	0	0	0	**0.011**	0.012	28.8

Table 7. Accuracy of FNF maps for Sumy region

Image data set	Forested area, thousands ha		Estimated area proportion	User's accuracy (commission errors)	Producer's accuracy (omission errors)	Overall accuracy
	Mapped (pixel area)	Estimated (Olofsson et. al, 2014)				
L30	559.8	531.6±36.2	0.223±0.015	0.909±0.051	0.956±0.039	0.896±0.023
S20	**606.1**	**569.3±30.5**	**0.239±0.013**	**0.926±0.047**	**0.989±0.019**	**0.906±0.024**
S10	594.0	569.3±32.5	0.239±0.014	0.933±0.045	0.971±0.031	0.907±0.023

L30 – Landsat 30-m; S20 – Sentinel 20-m; S10 – Sentinel 10-m.

The CCDC-based approach allowed us to map forested area dynamics using a single classification model. Since the approach utilized temporally smoothed TS, the obtained results can be more consistent in time than in the case of yearly mosaics.

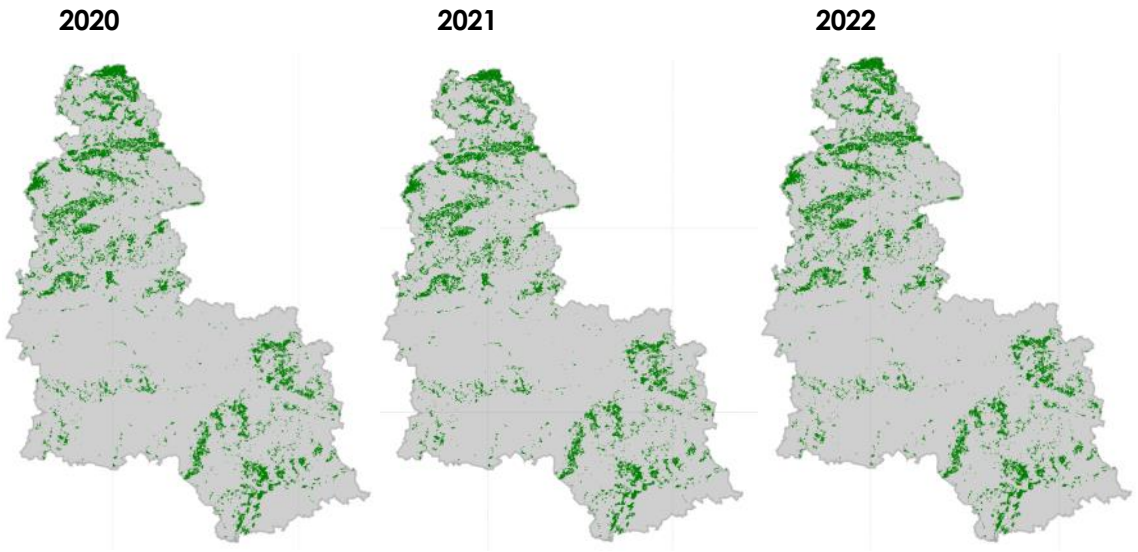

Figure 7. Dynamics of forested area extracted from Sentinel 2 (20-m) TS.

2.2. Tree species maps

2.2.1. Species presence/absence maps

The prediction of species distribution (see examples in Fig. 8) imputed using the threshold of BA > 1 $m^2 \cdot ha^{-1}$ performed well (Kappa > 0.3) for all species group except of rare species (Table 8). This can be explained by the fact that BAs for such species are typically lower than the selected threshold.

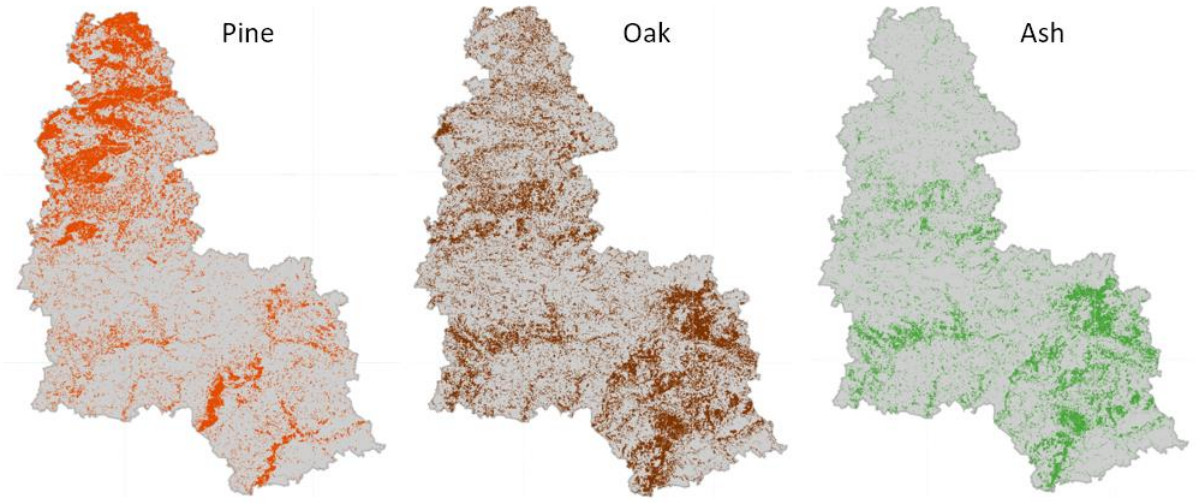

Figure 8. Presence/absence maps for major species within the Sumy region.

Table 8. Accuracy of tree species mapping (presence/absence) based on GNN imputation model (*k* = 3)

Species group	Prevalence	Number of observations		Cohen's kappa
		OP/PP	OA/PP	
		OP/PA	OA/PA	
Oak	0.497	45 27	12 61	0.461
Pine	0.559	64 17	4 60	0.712
Maple	0.289	26 16	8 95	0.574
Linden	0.276	16 24	10 95	0.342
Birch	0.269	20 19	11 95	0.437
Ash	0.317	23 23	4 95	0.517
Poplar	0.172	11 14	6 114	0.447
Alder	0.097	5 9	4 127	0.389
Willow	0.069	5 5	2 133	0.563
Other hardwood deciduous species	0.345	25 25	11 84	0.411
Deciduous 1 (maple, ash, linden)	0.448	46 19	7 73	0.631
Deciduous 2 (birch, poplar, alder, willow)	0.434	39 24	12 70	0.483

OP/PP = Observed Present / Predicted Present; OA/PP = Observed Absent / Predicted Present

OP/PA = Observed Present / Predicted Absent; OA/PA = Observed Absent / Predicted Absent

2.2.2. Map of dominant species

Two approaches were tested to create map of dominant species, i.e., (i) using GNN-imputed values of BA at pixel level and (ii) using discrete RF-classification.

The GNN imputation can simultaneously predict BAs for the list of species that were observed on the plot. This ability was used to identify the dominant species using predicted BA. Detailed examination of the GNN model showed some limitations in terms of its ability to accurately predict BA of individual species (Fig. 9). That is mostly true for species that often occupy similar ecological niches (e.g., ash, maple, linden). Extracting BA of individual species from such forest structures can be difficult, thus, model for broader species groups showed better performance (Table 9).

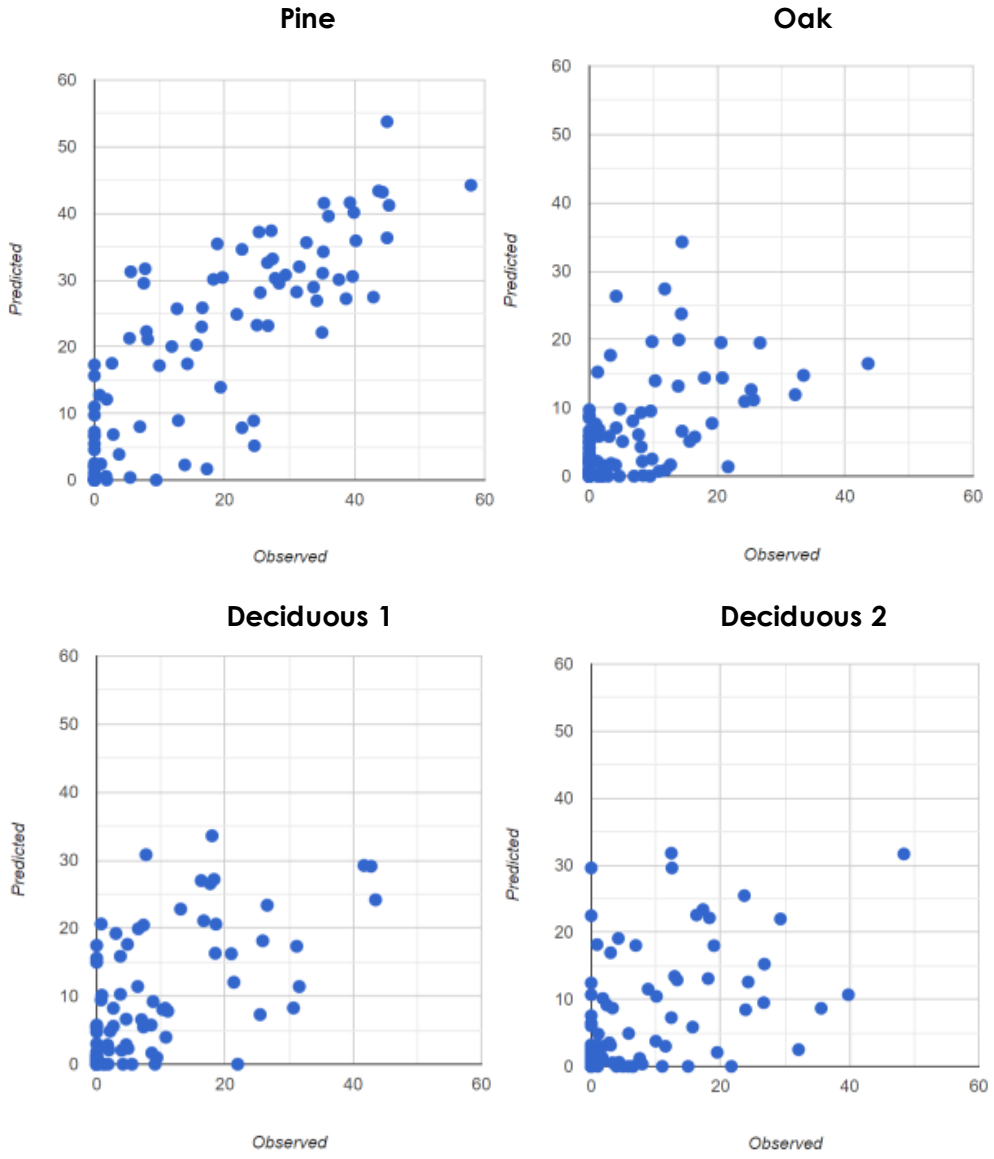

Figure 9. Predicted vs observed values of BA for species groups.

Table 9. Accuracy of BA prediction for species groups within the Sumy region using GNN imputation model (*k* = 3)

Species (species group)	R-squared
Pine	0.76
Oak	0.32
Deciduous 1 (maple, ash, linden)	0.44
Deciduous 2 (birch, poplar, alder, willow)	0.24

After detailed examination of the map errors in terms of obtained confidence intervals of mapped areas for each species group, an alternative approach was applied using RF classification. First, dominant species (with maximum BA) were identified for each NFI plot. Second, established dominant species were treated as discreate classes in the classification.

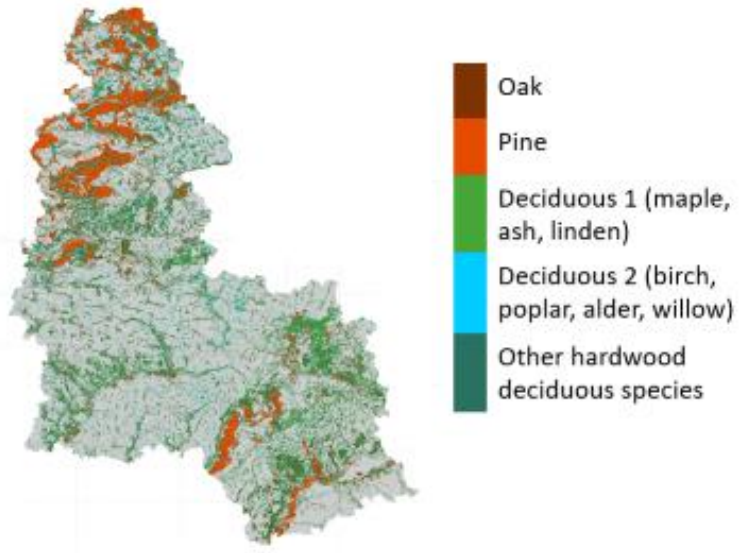

Figure 10. Map of the dominant species within the Sumy region extracted using RF-classification.

2.3. Mapping forest attributes

The effectiveness of mapping GSV (Fig. 11) is associated with the predictive performance of the GNN model for BA. This can be explained by a strong correlation between GSV and BA, while evaluation of the model for BA can be more explicit since it is not influenced by the accuracy of volume equations used to calculate GSV. Other forest attributes can also be predicted using the same nearest neighbor raster. Comparison of predicted and observed values of forest attributes at sample plot locations (Fig. 12) showed that data can be rather scattered. One can expect obtaining a better accuracy at a higher aggregation scale (e.g., 5×5 km grid) which was shown by (Myroniuk et al., 2022).

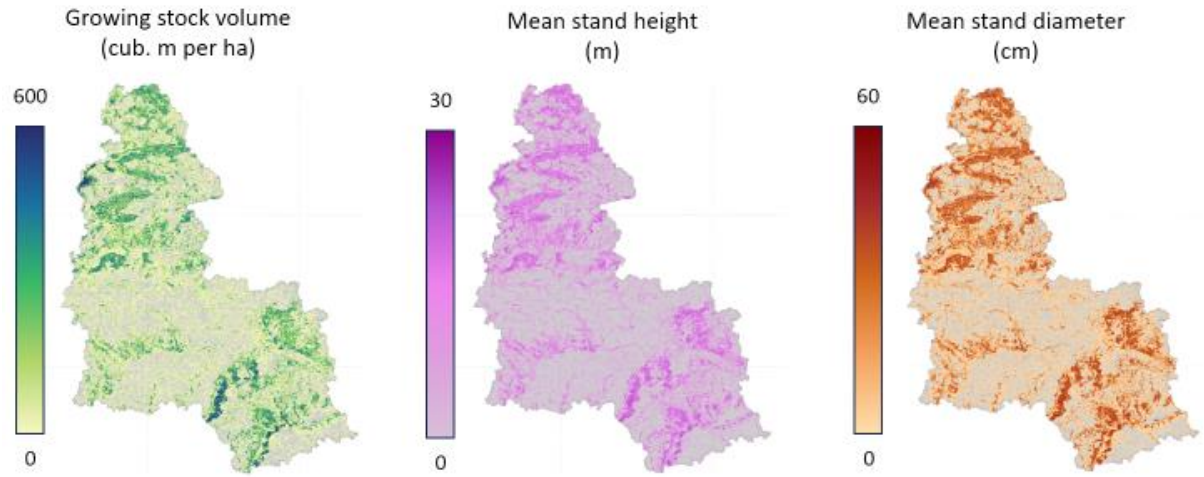

Figure 11. Maps of quantitative forest attributes within the Sumy region.

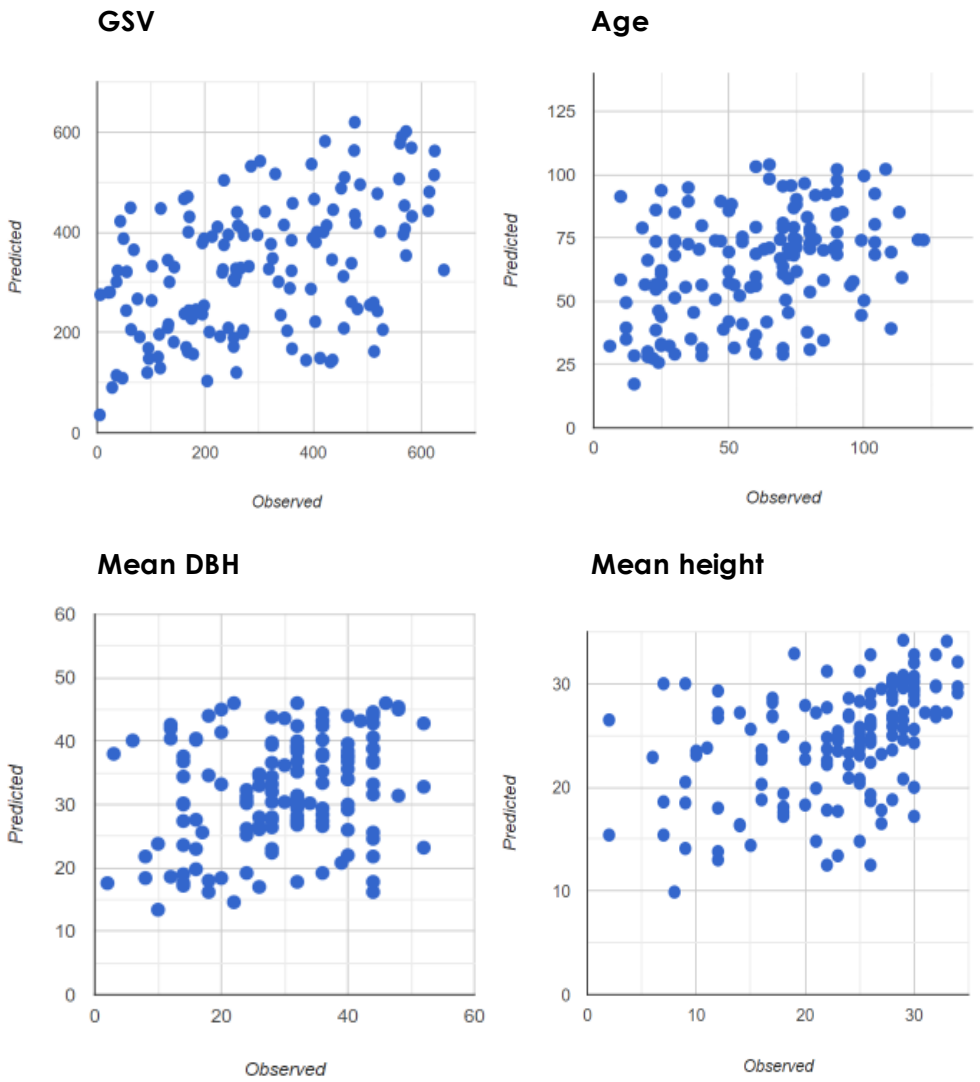

Figure 12. Predicted vs observed values of key forest attributes using NFI reference data.

2.4. Role of FMP data in the RS-Inventory

Traditionally, NFI is a source of independent information that is collected on sample plots. The proposed methodology of the RS-Inventory is a trade-off between the need for spatially explicit estimates of forest attributes and available field data. NFI data for large territories have never existed in Ukraine and cannot be collected because of safety reasons. Thus, historical FMP data can be the only available source of reference data to train models for such territories.

The study demonstrated certain potential for the combined use of NFI and FMP in RS-Inventory. BA estimates obtained for the same stands showed no systematical errors, however, high variability (Fig. 13).

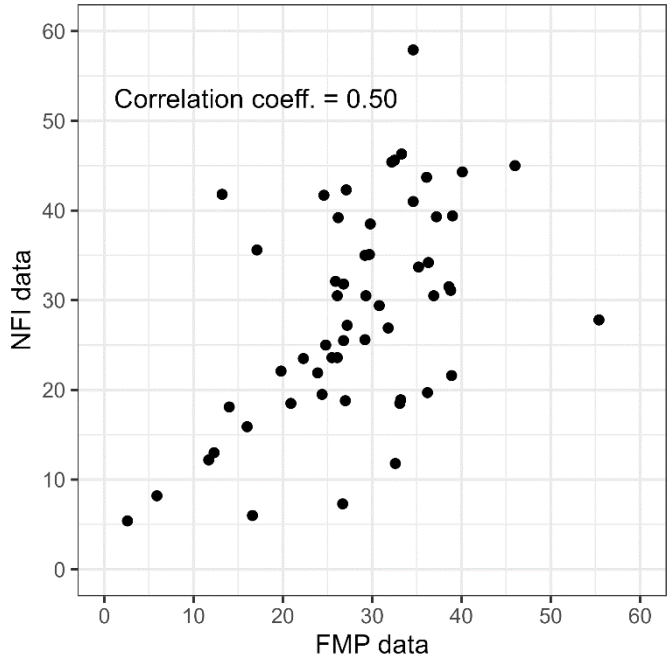

Figure 13. Relationship between BA estimated of sampled forest stands (n = 96) during FMP (2018) and NFI (2021).

Similar to NFI, selected 96 stands from FMP data were used to predict the forest attributes (Fig. 14). The distribution of observed and predicted data was more scattered than in the case of NFI data. Additionally, the overestimation of observations at the beginning of the data ranges indicated potential limitations of field data collection during FMP where visual estimates prevail over measurements. Thus, it is not recommended to combine FMP and NFI data for regions with available plots observations. The most effective approach would be the utility of FMP data only for regions lacking NFI plots.

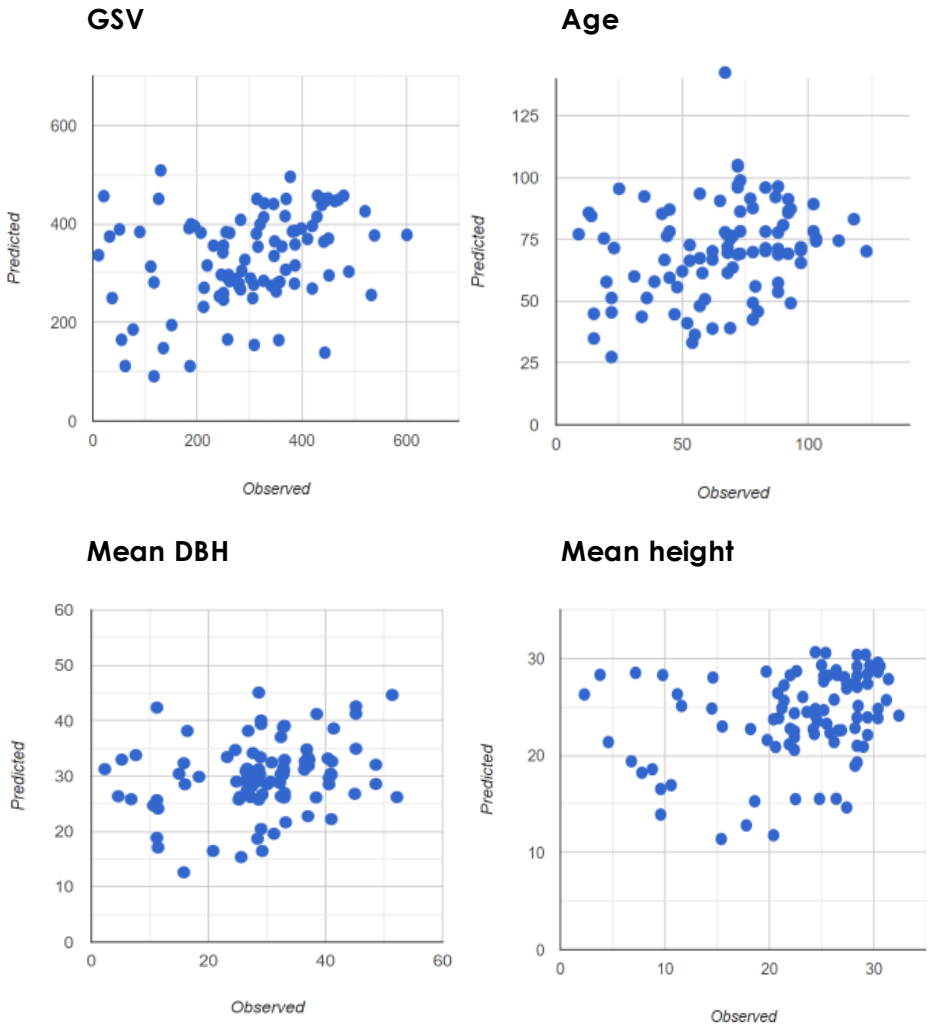

Figure 14. Predicted vs observed values of key forest attributes using FMP reference data.

2.5. RS-Inventory estimates

2.5.1. Forested area estimates for sub-population units

Forested area for sub-pollutions units with 95% confidence intervals can be obtained using the pixel area and the corresponding confusion matrix (see Table 5). As an example, Table 10 and Table 11 provide estimates for the administrative districts and community (territorial hromadas) levels.

Table 10. Distribution of forested area (with 95% confidence intervals) within administrative districts of the Sumy region

Administrative district (Capital city)	Forested area, thousands ha	Proportion of forested area
Konotop	118.8±6.4	0.229±0.012
Okhtyrka	73.5±4.0	0.230±0.012
Romny	60.5±3.5	0.156±0.009
Sumy	136.6±7.5	0.210±0.012
Shostka	179.9±9.3	0.355±0.018

Table 11. Distribution of forested area (with 95% confidence intervals) within territorial hromadas of the Sumy region

Official code of the territorial hromada	Ukrainian name of the territorial hromada	Forested area, thousands ha	Proportion of forested area
UA59060010000042952	Андріяшівська	10,9±0,6	0.180±0.010
UA59100010000064812	Березівська	15,3±0,8	0.331±0.017
UA59080010000078468	Бездрицька	2,9±0,2	0.376±0.020
UA59040010000075530	Боромлянська	7,1±0,4	0.231±0.012
UA59020010000024157	Бочечківська	12,1±0,6	0.318±0.017
UA59080030000075526	Білопільська	5,8±0,4	0.106±0.007
UA59020030000072865	Буринська	8,6±0,6	0.096±0.007
UA59080050000061215	Верхньосироватська	5,0±0,3	0.283±0.015
UA59040030000060142	Великописарівська	6,6±0,4	0.129±0.008
UA59080070000062635	Ворожбянська	1,5±0,1	0.102±0.007
UA59060030000069916	Вільшанська	4,1±0,2	0.156±0.009
UA59040050000033127	Грунська	5,7±0,3	0.235±0.013
UA59100030000078744	Глухівська	12,2±0,6	0.268±0.014
UA59100050000059594	Дружбівська	5,7±0,3	0.447±0.023
UA59020050000012539	Дубов'язівська	4,6±0,3	0.088±0.006
UA59100070000019079	Есманьська	9,8±0,6	0.178±0.010
UA59100090000041284	Зноб-Новгородська	22,0±1,1	0.415±0.021
UA59060050000060884	Коровинська	4,4±0,2	0.230±0.012
UA59040090000041737	Комишанська	2,2±0,1	0.171±0.010
UA59020070000032449	Конотопська	1,5±0,1	0.147±0.009
UA59080090000092991	Краснопільська	27,3±1,4	0.281±0.015
UA59020090000085438	Кролевецька	49,3±2,5	0.384±0.020
UA59040070000045520	Кириківська	2,8±0,2	0.103±0.007
UA59080110000034361	Лебединська	44,5±2,4	0.270±0.014
UA59060070000040784	Липоводолинська	5,0±0,4	0.085±0.006
UA59080170000056499	Миропільська	7,0±0,4	0.234±0.014
UA59080130000022249	Миколаївська	4,3±0,3	0.082±0.006
UA59080150000013842	Миколаївська1	2,6±0,2	0.095±0.007
UA59060090000012687	Недригайлівська	9,8±0,6	0.167±0.009
UA59020110000066430	Новослобідська	14,3±0,8	0.277±0.015
UA59080190000095280	Нижньосироватська	1,9±0,1	0.116±0.009
UA59040110000026694	Охтирська	3,0±0,2	0.357±0.019
UA59020130000060377	Попівська	15,0±0,9	0.168±0.010
UA59020150000078955	Путивльська	13,5±0,8	0.229±0.013
UA59060110000049734	Роменська	17,0±1,0	0.175±0.010
UA59080210000075243	Річківська	2,2±0,2	0.097±0.007
UA59080230000084731	Садівська	6,0±0,3	0.185±0.011
UA59100110000012703	Свеська	10,6±0,6	0.357±0.019
UA59100130000041016	Середино-Будська	27,6±1,4	0.466±0.024
UA59060130000041204	Синівська	3,8±0,2	0.128±0.008
UA59080250000082875	Степанівська	1,3±0,1	0.067±0.006
UA59080270000073662	Сумська	12,0±0,6	0.345±0.018
UA59040130000041676	Тростянецька	26,6±1,4	0.338±0.017
UA59080290000021284	Хотінська	2,1±0,2	0.087±0.007
UA59060150000055022	Хмелівська	5,5±0,3	0.143±0.008
UA59040150000076482	Чернеччинська	14,3±0,8	0.243±0.013
UA59040170000054314	Чупахівська	5,4±0,3	0.196±0.011
UA59100150000074932	Шалигинська	7,1±0,4	0.258±0.014
UA59100170000093676	Шосткинська	45,1±2,3	0.359±0.019
UA59080310000049988	Юнаківська	10,0±0,5	0.290±0.015
UA59100190000010734	Ямпільська	24,6±1,3	0.471±0.024

The map of dominant species (Figure 10) was used to extract pixel areas for the corresponding species groups. The mapped (pixel) areas for each group were adjusted using the ratio between estimated and mapped total forested area. The confidence intervals for area occupied by dominant species were derived using the "good practice" approach (Olofsson et al., 2014) and obtained LOO error matrix.

Forested area estimates were also provided for age groups of forest stands. To reduce potential errors, 40-year age intervals were used (Table 13).

Table 12. Area of forest stand by groups of dominant species (with 95% confidence intervals)

Species group	Estimated (Olofsson et al., 2014)	
	Area	Proportion
Oak	101.3±35.0	0.178±0.061
Pine	213.0±25.1	0.374±0.044
Deciduous 1 (maple, ash, linden)	103.0±34.0	0.181±0.060
Deciduous 2 (birch, poplar, alder, willow)	107.6±35.8	0.189±0.063
Other hardwood deciduous species	44.4±25.0	0.078±0.044
Total	569.3±30.5	0.239±0.013

Table 13. Area of forest stands by 40-year age groups

Age group	Forested area (pixel area), thousand ha
40 years and younger	143.4
41-80 years	362.9
81 year and older	99.8
Total	606.1

2.5.2. Mean values of forest attributes

Mean values of forest attributes were derived using the GREG estimator (Table 13). The developed model residuals for all attributes had negative values. They were applied to adjust mean values calculated from the maps. Confidence intervals were compiled using model-assisted estimates and standard errors (calculated as 1.98 × the square root of variances).

Table 14. Model-assisted estimates and confidence intervals for quantitative forest attributes

	Sample-based mean		Map-derived mean	GREG		
Forest attribute	Observed (*n* = 145)	Predicted (*n* = 145)	(*N* = 24193140)	Model residuals	Variance	95% CI
Age (years)	60	64	60	-4	5.7	56±5
DBH (cm)	29.7	32.0	29.9	-2.3	1.03	27.6±2.0
HT (m)	23.0	24.4	22.9	-1.4	0.35	21.5±1.2
BA ($m^2 \cdot ha^{-1}$)	27.7	29.0	27.7	-1.3	1.05	26.4±2.0
GSV ($m^3 \cdot ha^{-1}$)	308	334	305	-26	192	282±27

Maps of dominant species and age groups were used to extract mean values of forest attributes (Table 14, Table 15). Confidence intervals for mean values of forest attributes within groups of dominant species were derived using residuals and estimated variances of the models (see Table 13). Given the predictive performance of the GNN model, the selection of narrow age classes (e.g., 10-year intervals) could cause significant uncertainties in the estimates. Thus, the decision was made in favor of broad 40-year age groups.

Table 15. Mean values of forest attributes by groups of dominant species

Species group	Age, years	DBH, cm	HT, m	BA, $m^2 \cdot ha^{-1}$	GSV, $m^3 \cdot ha^{-1}$
Oak	66±5	30.3±2.0	23.1±1.2	27.8±2.0	309±27
Pine	57±5	30.5±2.0	23.5±1.2	29.2±2.0	332±27
Deciduous 1 (maple, ash, linden)	64±5	30.0±2.0	23.6±1.2	26.9±2.0	295±27
Deciduous 2 (birch, poplar, alder, willow)	55±5	28.6±2.0	21.4±1.2	25.8±2.0	225±27

Table 16. Mean values of forest attributes by 40-year age groups

Age group	Age, years	DBH, cm	HT, m	BA, $m^2 \cdot ha^{-1}$	GSV, $m^3 \cdot ha^{-1}$
40 years and younger	31	19	15	21	165
41-80 years	63	32	25	29	330
81 year and older	90	38	28	33	417

TABLES

FIGURES

CONCLUSIONS

The case study for the Sumy region demonstrated the advantages of the RS-Inventory in a situation when only limited field data are available. Apart from design-based forest inventory, the proposed approach provides foundations for both forest mapping and forest assessment. In this regard, the RS-Inventory overperforms the traditional sample-based forest inventory. However, the case study also revealed some limitations of the approach due to different factors affecting the accuracy of predictive models.

First, this study was based on a limited number of observations that are not sufficient to provide reliable enough estimates using design-based neither model assisted approaches. To increase the efficiency of the proposed approach, the sample size of reference observations needs to be increased. Thus, there are strong arguments for *processing data for larger than one region of territories*. Combining field data from adjacent regions can be a possible solution to address this issue.

Second, misregistration of the coordinates of plot centers may be also an issue. High-resolution imagery can be used to remove plots that have obvious errors with coordinates. The plots that straddle different forest stands or land cover categories could also impact the accuracy of the modeling. The importance of this problem is higher as forest fragmentation increases. Overall, it is recommended *not to include plots located on edges of forest stands into reference data sets or make such decisions based on visual inspection of each plot using high-resolution images*.

Third, the study showed that the performance of the models improves for groups of species. There are only general recommendations for grouping can be provided because forest structure in Ukraine is different. Thus, *species should be combined into groups if they occupy similar ecological niches* (e.g., species growing in mixture stands).

Forth, the accuracy assessment in this study was performed at 20-m pixel-level, while most forest management decisions are made at least at stand-level. From this perspective, *the accuracy of the models will be better for a higher aggregation scale*.

Fifth, the concept of RS-Inventory that utilized temporally fitted TS of satellite images assumes incorporating all available historical field-sampled data. It is expected *to achieve better performance of models incorporating both historical and newly collected sample plots.*

ANNEXES

ANNEX 1. PARAMETERS OF THE FOREST LIVE BIOMASS (EQ. (A1))

Live biomass fraction	Equation (A1) parameter estimation (Bilous et al., 2017)						RMSD
	$\hat{a}_0$	$\hat{a}_1$	$\hat{a}_2$	$\hat{a}_3$	$\hat{a}_4$	$\hat{a}_5$	
	Pine (Shvidenko et al., 2007)						
Stem	0.26990	0.08399	0.14600	0.00984	-0.00113	-0.10480	0.069
Branches	0.27380	-0.73450	0.71230	-0.07102	0.00429	-0.33160	0.033
Foliage	0.43760	-1.14000	1.23500	0.41980	0.00307	-0.77010	0.023
Tree roots	0.05534	-0.21860	0.64560	-0.32960	0.00045	0.32010	0.061
GFF	0.03920	0.66900	0.14100	-1.70000	-0.00396	-0.92000	1.576
Understory	0.00258	2.65800	-0.82430	0.74390	-0.01512	-1.97200	1.384
	Birch						
Stem	0.43850	0.04412	-0.01376	-0.07286	-0.00064	0.00796	0.061
Branches	0.01383	-0.02150	0.18670	-1.43800	0.00113	1.09400	0.038
Foliage	0.04388	-0.72620	0.35420	-0.92660	0.00392	0.96070	0.018
Tree roots	0.22690	-0.48550	1.08200	0.42080	0.00580	-0.62770	0.053
GFF	88.1900	-0.36490	0.31670	2.35500	0.02050	-4.43900	1.576
Understory	0.68430	1.14400	0.95050	3.32300	-0.00634	-5.28500	1.384
	Black alder						
Stem	0.42310	0.03063	-0.03498	-0.01347	-0.00002	0.00003	0.036
Branches	0.01997	-0.44310	0.99660	-0.65910	0.00361	0.20570	0.013
Foliage	0.00679	-0.62360	1.34800	-0.88740	-0.00601	0.33290	0.005
Tree roots	1.50300	-0.39290	0.56250	1.45300	0.00320	-2.40900	0.044
GFF	12.5400	0.42700	0.42800	2.75400	0.00073	-4.30100	1.048
Understory	0.00032	1.06800	0.21400	-3.24500	-0.00298	3.95100	0.635
	Aspen						
Stem	0.44380	-0.02559	0.02371	-0.00506	0.00047	-0.00777	0.066
Branches	0.16980	-0.35910	0.48230	0.79180	0.00725	-0.47330	0.028
Foliage	0.01652	-0.72700	0.71050	-0.92820	-0.00049	1.27100	0.005
Tree roots	1.06900	-0.33720	0.24350	0.73940	0.00070	-1.18500	0.043
GFF	84.1800	-0.08300	0.56000	2.72600	0.01110	-5.51200	1.766
Understory	0.98800	0.35000	0.50300	1.42400	0.01100	-1.99600	2.731
	Oak (Shvidenko et al., 2007)						
Stem	0.57400	-0.04679	0.09587	0.02519	0.00080	-0.01498	0.082
Branches	0.03194	-0.44630	1.25300	-0.60530	0.00193	0.61700	0.075
Foliage	0.01828	-0.35940	0.89200	-0.15230	-0.00776	0.32760	0.012
Tree roots	0.07831	-0.62020	1.46700	-0.30380	0.00316	0.30390	0.094
GFF	0.18870	0.05998	0.60810	-1.73500	0.00051	0.92440	1.790
Understory	0.00033	2.13900	-0.40800	-1.83300	-0.01794	2.12700	1.735

Live biomass of all the forest stands can be estimated as follows:

$$R_{fr} = {}^{M_{fr}}/_{GSV} = a_0 + A^{a_1} \cdot SI^{a_2} \cdot RSt^{a_3} \cdot \exp(a_4 \cdot A + a_5 \cdot RSt), \qquad (A1)$$

where R_{rf} is the biomass expansion factor; M_{fr} is the live biomass of fraction *fr*, oven-dry t ha^{-1}; GSV is the growing stock volume in m^3; *A* is age in years; RSt is relative stocking; SI is the site index, which reflects the quality of the site (Shvidenko et al., 2007); and a_0-a_5 are model parameters.

REFERENCES

1. ABATZOGLOU, J. T., DOBROWSKI, S. Z., PARKS, S. A., & HEGEWISCH, K. C. (2018). TERRACLIMATE, A HIGH-RESOLUTION GLOBAL DATASET OF MONTHLY CLIMATE AND CLIMATIC WATER BALANCE FROM 1958–2015. SCIENTIFIC DATA, 5(1), 170191. HTTPS://DOI.ORG/10.1038/SDATA.2017.191
2. BEY, A., SÁNCHEZ-PAUS DÍAZ, A., MANIATIS, D., MARCHI, G., MOLLICONE, D., RICCI, S., BASTIN, J.-F., MOORE, R., FEDERICI, S., REZENDE, M., PATRIARCA, C., TURIA, R., GAMOGA, G., ABE, H., KAIDONG, E., & MICELI, G. (2016). COLLECT EARTH: LAND USE AND LAND COVER ASSESSMENT THROUGH AUGMENTED VISUAL INTERPRETATION. REMOTE SENSING, 8(10), 807. HTTPS://DOI.ORG/10.3390/RS8100807
3. BILOUS, A. M., KASHPOR, S. M., MYRONIUK, V. V., SVYNCHYK, V. A., & LESNIK, O. M. (EDS.). (2020). FOREST INVENTORY HANDBOOK. DNIPRO: LIRA LTD, 2020, 364 [IN UKRAINIAN].
4. BILOUS, A., MYRONIUK, V., HOLIAKA, D., BILOUS, S., SEE, L., & SCHEPASCHENKO, D. (2017). MAPPING GROWING STOCK VOLUME AND FOREST LIVE BIOMASS: A CASE STUDY OF THE POLISSYA REGION OF UKRAINE. ENVIRONMENTAL RESEARCH LETTERS, 12(10), 13. HTTPS://DOI.ORG/10.1088/1748-9326/AA8352
5. BREIMAN, L. (2001). RANDOM FORESTS. MACHINE LEARNING, 45(1), 5–32. HTTPS://DOI.ORG/10.1023/A:1010933404324
6. CRIST, E. P., & CICONE, R. C. (1984). COMPARISONS OF THE DIMENSIONALITY AND FEATURES OF SIMULATED LANDSAT-4 MSS AND TM DATA. REMOTE SENSING OF ENVIRONMENT, 14(1–3), 235–246. HTTPS://DOI.ORG/10.1016/0034-4257(84)90018-X
7. FOGA, S., SCARAMUZZA, P. L., GUO, S., ZHU, Z., DILLEY, R. D., BECKMANN, T., SCHMIDT, G. L., DWYER, J. L., JOSEPH HUGHES, M., & LAUE, B. (2017). CLOUD DETECTION ALGORITHM COMPARISON AND VALIDATION FOR OPERATIONAL LANDSAT DATA PRODUCTS. REMOTE SENSING OF ENVIRONMENT, 194, 379–390. HTTPS://DOI.ORG/10.1016/J.RSE.2017.03.026
8. GORELICK, N., HANCHER, M., DIXON, M., ILYUSHCHENKO, S., THAU, D., & MOORE, R. (2017). GOOGLE EARTH ENGINE: PLANETARY-SCALE GEOSPATIAL ANALYSIS FOR EVERYONE. REMOTE SENSING OF ENVIRONMENT, 202, 18–27. HTTPS://DOI.ORG/10.1016/J.RSE.2017.06.031
9. KEY, C. H., & BENSON, N. C. (2006). LANDSCAPE ASSESSMENT (LA): SAMPLING AND ANALYSIS METHODS (GENERAL TECHNICAL REPORT RMRS-GTR-164; FIREMON: FIRE EFFECTS MONITORING AND INVENTORY SYSTEM, P. LA-1-LA-51). ROCKY MOUNTAIN RESEARCH STATION, US DEPARTMENT OF AGRICULTURE, FOREST SERVICE.
10. MATSALA, M., MYRONIUK, V., BORSUK, O., VISHNEVSKIY, D., SCHEPASCHENKO, D., SHVIDENKO, A., KRAXNER, F., & BILOUS, A. (2023). WALL-TO-WALL MAPPING OF CARBON LOSS WITHIN THE CHORNOBYL EXCLUSION ZONE AFTER THE 2020 CATASTROPHIC WILDFIRE. ANNALS OF FOREST SCIENCE, 80(1), 26. HTTPS://DOI.ORG/10.1186/S13595-023-01192-W

11. MCCONVILLE, K. S., MOISEN, G. G., & FRESCINO, T. S. (2020). A TUTORIAL ON MODEL-ASSISTED ESTIMATION WITH APPLICATION TO FOREST INVENTORY. FORESTS, 11(2), 244. HTTPS://DOI.ORG/10.3390/F11020244

12. MYRONIUK, V., BELL, D. M., GREGORY, M. J., VASYLYSHYN, R., & BILOUS, A. (2022). UNCOVERING FOREST DYNAMICS USING HISTORICAL FOREST INVENTORY DATA AND LANDSAT TIME SERIES. FOREST ECOLOGY AND MANAGEMENT, 513, 120184. HTTPS://DOI.ORG/10.1016/J.FORECO.2022.120184

13. OHMANN, J. L., & GREGORY, M. J. (2002). PREDICTIVE MAPPING OF FOREST COMPOSITION AND STRUCTURE WITH DIRECT GRADIENT ANALYSIS AND NEAREST- NEIGHBOR IMPUTATION IN COASTAL OREGON, U.S.A. CANADIAN JOURNAL OF FOREST RESEARCH, 32(4), 725–741. HTTPS://DOI.ORG/10.1139/X02-011

14. OLOFSSON, P., FOODY, G. M., HEROLD, M., STEHMAN, S. V., WOODCOCK, C. E., & WULDER, M. A. (2014). GOOD PRACTICES FOR ESTIMATING AREA AND ASSESSING ACCURACY OF LAND CHANGE. REMOTE SENSING OF ENVIRONMENT, 148, 42–57. HTTPS://DOI.ORG/10.1016/J.RSE.2014.02.015

15. SHVIDENKO, A., SCHEPASCHENKO, D., NILSSON, S., & BOULOUI, Y. (2007). SEMI-EMPIRICAL MODELS FOR ASSESSING BIOLOGICAL PRODUCTIVITY OF NORTHERN EURASIAN FORESTS. ECOLOGICAL MODELLING, 204, 163–179.

16. WEISS, A. (2001). TOPOGRAPHIC POSITION AND LANDFORMS ANALYSIS. [POSTER PRESENTATION]. ESRI USER CONFERENCE, SAN DIEGO, CA.

17. ZHU, Z., & WOODCOCK, C. E. (2014). CONTINUOUS CHANGE DETECTION AND CLASSIFICATION OF LAND COVER USING ALL AVAILABLE LANDSAT DATA. REMOTE SENSING OF ENVIRONMENT, 144, 152–171. HTTPS://DOI.ORG/10.1016/J.RSE.2014.01.011